

Research

Simulation and Implementation of a Porous Silicon Reflector for Epitaxial Silicon Solar Cells

Filip Duerinckx^{*,†}, Izabela Kuzma-Filipek, Kris Van Nieuwenhuysen, Guy Beaucarne and Jef Poortmans
IMEC vzw, Kapeldreef 75, B-3001 Heverlee, Belgium

One of the main challenges in the ongoing development of thin film crystalline silicon solar cells on a supporting silicon substrate is the implementation of a long-wavelength reflector at the interface between the epitaxial layer and the substrate. IMEC has developed such a reflector based on electrochemical anodization of silicon to create a multi-layer porous silicon stack with alternating high and low porosity layers. This innovation results in a 1–2% absolute increase in efficiency for screenprinted epitaxial cells with a record of 13.8%. To reach a better understanding of the reflector and to aid in its continued optimization, several extensive optical simulations have been performed using an in-house-developed optical software programme. This software is written as a Microsoft Excel workbook to make use of its user-friendliness and modular structure. It can handle up to 15 individual dielectric layers and is used to determine the influence of the number and the sequence of the layers on the internal reflection. A sensitivity analysis is also presented. A study of the angle at which the light strikes the reflector shows separate regions in the physical working of the reflector which include a region where the Bragg effect is dominant as well as a region where total internal reflection plays the largest role. The existence of these regions is proved using reflection measurements. Based on these findings, an estimate is made for the achievable current gain with an ideal reflector and the potential of epitaxial silicon solar cells is determined. Copyright © 2008 John Wiley & Sons, Ltd.

KEY WORDS: porous silicon; optical simulation; light confinement; epitaxy; screen printing

Received 11 July 2007; Revised 10 December 2007

INTRODUCTION

The recent shortage of silicon feedstock and related increase in prices for electronic grade silicon has resulted in a strong response from the photovoltaic community. Accelerated efforts by feedstock suppliers, research centres, equipment manufacturers and PV companies to find an answer to this problem have led to

advances on several levels: an increased availability of Electronic Grade silicon, the strong appearance of solar grade feedstock, the research towards the use of thinner silicon wafers and cells and a new emphasis on high efficiency technologies. All have the aim of reducing the silicon material cost by diminishing the amount of silicon used per produced Wattpeak (Wp) and/or by making use of less pure but cheaper silicon.

Besides IMEC's research towards the use of thinner cells, as made evident in the successful i-PERC approach on thin multi- and monocrystalline wafers,¹ a lot of emphasis is put on so-called next generation

* Correspondence to: Filip Duerinckx, IMEC vzw, Kapeldreef 75, B-3001 Heverlee, Belgium.

† E-mail: filip.duerinckx@imec.be

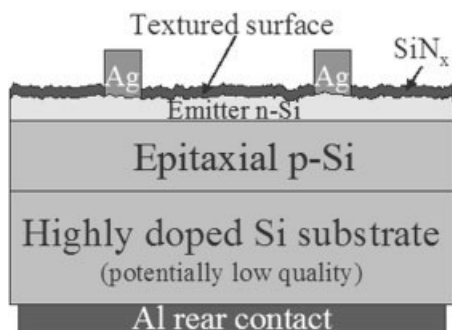


Figure 1. Cross-section of a screenprinted epitaxial cell

technologies. A prime example is the development of technology for epitaxial thin film crystalline silicon solar cells² which is the topic of this paper. This technology is based on the use of a low-cost, low-quality silicon substrate which only serves as a carrier but is not electrically active. The substrate can be a sawn wafer, or preferably, a high-throughput ribbon made from slightly upgraded metallurgical silicon. The active layer is grown on top of the substrate by epitaxy using either atmospheric pressure or low pressure chemical vapour deposition (APCVD or LPCVD)³ followed by texturing of the front surface, emitter diffusion, deposition of an anti-reflective coating and finally printing and firing of the contacts. The stack of substrate and epitaxial layer is called a wafer equivalent⁴ since it can be processed as a regular bulk silicon wafer into a solar cell using state-of-the-art production lines. Figure 1 shows the cross-section of a standard epitaxial silicon solar cell which looks indeed very similar to a typical screen printed multi- or monocrystalline silicon solar cell. This can be an important advantage for industrial implementation.

This paper addresses one of the most important drawbacks of this type of cell, namely the limited efficiency of the standard epitaxial cell. This drawback can be attributed to the lack of light trapping at the interface between the epitaxial layer and the substrate in the cell of Figure 1. Since the epitaxial layer has a limited thickness of only 20 μm , a large portion of the light in the range from 750 nm to 1100 nm will not be absorbed on the first pass through the epitaxial layer and will be lost in the highly doped low-quality substrate if no internal reflector at the epi-substrate interface is foreseen. IMEC has developed a solution for this problem based on a multiple layer porous Si stack acting as a Bragg reflector. This stack of layers, sandwiched in between the silicon substrate and the

epitaxial layer, can reflect long wavelength light back into the active epitaxial layer. In combination with a diffusive textured surface on the front of the cell, this can lead to a drastically enhanced path length. Porous Si stacks and Bragg reflectors in general are finding more applications both in the world of photovoltaics (e.g. porous Si stacks to create 'black silicon',⁵ use of gratings and Bragg reflector as back surface reflector for solar cells⁶) and for optical devices in general.^{7,8}

The next chapter will present some of the achieved results. Although this approach has been very successful, there is a need for detailed optical calculations to understand and further optimize the beneficial effects of the internal reflector. To that aim, an optical calculation software was developed in-house to meet the necessary requirements of user friendliness and layer quantity. The latter refers to the porous silicon stack which can consist of 15 individual layers. The reasoning behind the software calculations will be explained (Section 'Software for Optical Simulation') followed by an analysis of the parameters influencing the efficiency of this porous silicon reflector (Section 'Simulation of a Porous Silicon Intermediate Reflector'). The outcome of these calculations together with other considerations will lead to a discussion of the potential of the epitaxial silicon solar cell (Section 'Potential of an Epitaxial Silicon Solar Cell').

THE EPITAXIAL SILICON SOLAR CELL: STATE-OF-THE-ART

The internal reflector for the epitaxial silicon solar cells consists of multiple porous silicon layers of alternating low and high porosity and is made by electrochemical anodization on the low quality, highly doped silicon substrate. During the subsequent epitaxial deposition at atmospheric pressure, the porous layers reorganize into quasi-monocrystalline silicon layers with large voids.⁹ This process is driven by a minimization of the surface energy.¹⁰ However, the original distribution of alternating layers is preserved (Figure 2): the original low porosity layer is transformed into a crystalline silicon of approximately the same thickness but with small voids. The diameter of these voids is typically in the 10–20 nm range. The originally high porosity silicon layer similarly is reorganized into a crystalline silicon layer with larger voids (diameter \sim 150 nm). This stack of layers is designed in such a way that the individual layers promote constructive interference for long

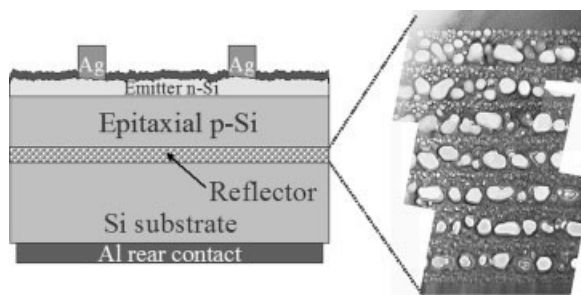


Figure 2. Cross-section of an epitaxial cell including porous silicon reflector

wavelength light (750–1100 nm). In other words, we aim to construct a Bragg reflector. In practice, this means that the relationship between the layer thickness d , the refractive index n and the design wavelength λ for maximal internal reflection is given by the quarter-wavelength rule:

$$d = \frac{\lambda}{4n} \quad (1)$$

More detailed information about the design process is available in a previous entry in this journal¹¹ and in other sources.³ Typically, the reflector stack consists of 15 individual layers with refractive indices of 2.3 and 3.0 for the layers with large and small voids, respectively. These refractive indices are estimated from a Maxwell-Garnier model of the individual reorganized layers.¹²

This reflector concept has been applied for epitaxial cells both on high quality monocrystalline substrates (reference case) and low quality multicrystalline substrates (final application case). For the former, top efficiencies of 13.8% have been obtained³ for small $4 \times 4 \text{ cm}^2$ screenprinted epitaxial cells (Table I). Reference cells without reflector typically reach 12.5–12.8% so there is a gain of 1% absolute in efficiency by inclusion of the internal reflector. Application on small multicrystalline UMG-Si substrates has likewise resulted in a top efficiency of

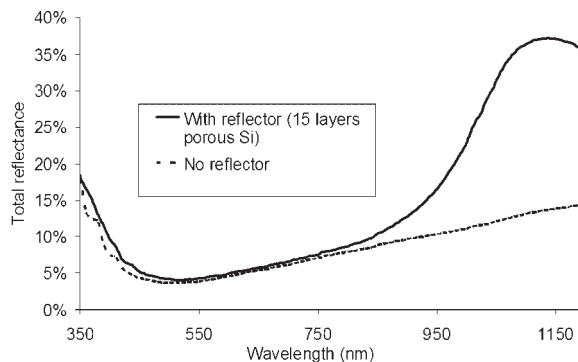


Figure 3. Comparison of external reflectance measured on epitaxial cells with and without porous Si internal reflector

13.5% using a screenprinted process. Recently a transfer of this technology to larger wafer sizes has been started. A first trial once more on UMG-Si has produced cells (size: $8.5 \times 8.5 \text{ cm}^2$) with an efficiency above 13% (Table I). The direct proof for the beneficial effect from the reflector is shown in Figure 3 depicting the measured reflectance of an epitaxial wafer (=substrate + epitaxial layer) with and without the inclusion of the internal reflector. The epitaxial surface is plasma textured in both cases resulting in a diffuse lambertian behaviour of the light travelling through the epitaxial layer. It is clear that the sample including the reflector has a high internal reflection which leads to the sharp increase in the external reflection measured for the long wavelength range. The internal reflection can be estimated from these measurements as described in Reference¹¹. Typically, an internal reflectance of 70–80% is extracted. Besides the aim of making an optical mirror in the middle of the device, the reflector should also be electrically transparent for majority carriers since the Al contact is made at the rear of the substrate. An analysis by SIMS, SRP and resistance measurements have demonstrated that this is no issue of concern.¹³

Although these results have clearly demonstrated the beneficial effect on short-circuit current and efficiency, optical simulations are needed for a better

Table I. Best screenprinted epitaxial thin film crystalline silicon solar cells on highly doped monocrystalline and upgraded metallurgical grade (UMG) silicon

| Substrate | Cell size (cm^2) | Jsc (mA/cm^2) | Voc (mV) | FF (%) | Eff. (%) |
|------------------------|-----------------------------|---------------------------------|----------|--------|----------|
| Mono-Si (highly doped) | 18 | 28.7 | 621 | 77.8 | 13.8 |
| UMG-Si | 18 | 28.7 | 606 | 77.7 | 13.5 |
| UMG-Si | 71 | 27.7 | 611 | 77.7 | 13.2 |

understanding of the optical effects and for further optimization of the stack. Towards this aim, it was decided to develop an optical calculation programme capable of handling a structure of 15 dielectric layers sandwiched by silicon on both sides. The reasoning behind this software is described in the following section.

SOFTWARE FOR OPTICAL SIMULATION

Most simulation programmes for calculation of specular reflection, transmission and absorption of multilayer optical problems rely on the matrix method.¹⁴ While straightforward to programme, we opted for a different method, the main reason being user-friendliness. Therefore it was opted to do the calculations in a single, large Microsoft Excel workbook so that all input and output information is available at the same place. Changing the thickness or optical parameters of a layer would then be nothing more than a copy/paste procedure. The output can be directly plotted by the graph functions available in Excel.

The method used is proposed in References¹⁵ and¹⁶. It relies on the fact that a dielectric coating can be described by an effective reflection coefficient and phase change. Such a thin film can then, for the purpose of the calculation, be replaced by a single interface with the same properties. By repeating the procedure for subsequent layers, one can work, layer by layer, through the whole stack till the boundary material is reached.

This procedure is illustrated in Figure 4 for the relatively simple case of a MgF₂/SiN_x Double Layer Anti-Reflective Coating (DLARC) on a silicon substrate for normal incidence of the impinging light. Each interface is described by a reflection factor (r_1 , r_2 , r_3) dependent on the complex refractive indices of both adjacent materials. The influence of the bottom SiN_x layer can be included in a new reflection factor (r_2^*) and is determined by the reflection factors of the two surrounding interfaces (r_1 , r_2) and the optical thickness of the layer. The nitride layer can then be removed from the system if the new reflection factor (r_2^*) is used at the MgF₂/Si interface, which is created for calculation purposes (see Figure 4). This leads to a new reflection factor (r_3^*) calculated from r_2^* , r_3 and the optical thickness of the MgF₂-layer. A single Air/Si interface with a reflection factor r_3^* remains, which is

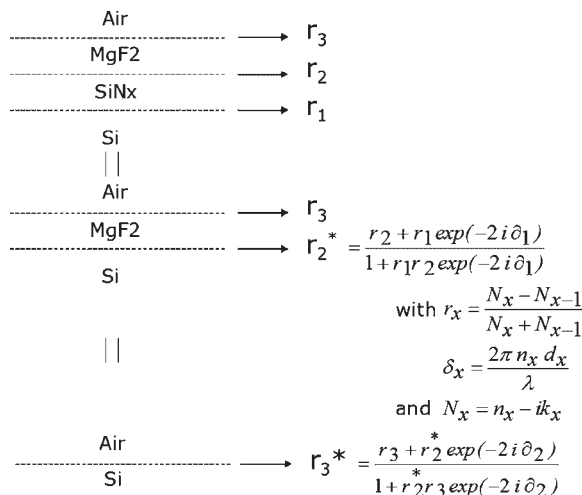


Figure 4. Procedure for calculation of the reflection factors for the case of a Double Layer ARC coating on silicon in the case of normal incidence (n_x and k_x are, respectively, the refractive index and extinction coefficient of layer 'x', d_x is its thickness and λ is the wavelength)

mathematically equivalent to the original structure. The reflectance is then simply the square of the modules of the complex number r_3^* . If the photons strike the interface at an angle, all formulas become dependent on the angle of the rays inside the layers, which can be calculated using a complex version of Snellius Law, and the procedure has to be done separately for parallel and perpendicular polarized light.

This procedure can be used for an unlimited amount of layers and is by definition a modular construction. An additional layer translates into an additional block of cells for calculation of the optical properties of this layer. This procedure has been introduced in a Microsoft Excel sheet and allows the calculation of the absorption, reflection and transmission ('ART') for any chosen wavelength range. The following parameters can be given as input:

- Thickness of dielectric layers.
- Refractive index of dielectric layers and surrounding media.
- Extinction coefficient of dielectric layers and surrounding media.
- Incident angle of light.

The ART-software can be used for any optical problem dealing with coatings (anti-reflection coatings, back surface reflectors, internal reflector) up to 15 individual layers, not including the surrounding media.

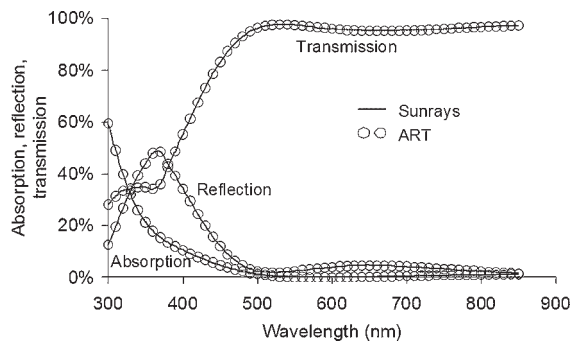


Figure 5. Comparison between Sunrays and ART for the simulation of a DLARC structure ($\text{MgF}_2/\text{SiN}_x/\text{Si}$) at normal incidence

It has been extensively tested and compared to other commercially available software. Figure 5 compares ART and SUNRAYS¹⁷ for the calculation of the reflection, transmission and absorption of the DLARC structure mentioned previously on a polished Si surface. The simulated structure incorporates a silicon rich silicon nitride layer which explains the high absorption at short wavelengths. The results of both programmes are identical. The same conclusion was reached for light incident at an angle. ART gives the possibility of easily extending the calculations to a 15-layer stack while Sunrays is limited to a stack of three dielectric layers.

SIMULATION OF A POROUS SILICON INTERMEDIATE REFLECTOR

A first interesting topic for the case of a porous Si intermediate reflector is the influence that the number of layers has on the internal reflection. The result for 3, 7, 11 and 15 layers of alternating low and high refractive index is shown in Figure 6. The design wavelength was 950 nm and the refractive indices of the layers were 2.35 and 3.05, respectively. The angle of incidence was 0 degree, so perpendicular to the interface. Clearly, a higher number of layers increases the internal reflection at the epi/reflector interface as expected for a Bragg reflector. A maximum achievable reflectance of 94.9% is reached for the 15-layer case. Remark that the shape of the reflected curve resembles a block shape for a high number of layers. In other words, the system behaves as a mirror for a well-defined wavelength range. The width of this

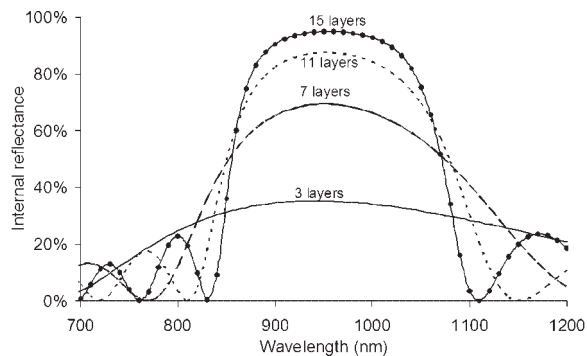


Figure 6. Influence of number of layers in the porous Si reflector on the internal reflectance and the stop-gap

stop-gap is approximately 215 nm from 855 to 1070 nm.

A higher number of layers (>15) will only marginally increase the reflection without impacting the stop-gap. The easiest method, at least theoretically, to improve the reflector is to widen the gap between the refractive indices of the layers. Figure 7 compares two reflectors: one consists of 15 layers with alternating refractive indices of 2.35 and 3.05, while the second reflector has refractive indices of 2.05 and 3.05. These are the refractive indices after reorganization of the porous Si stack. In practice, this would mean a difference in the porosity of the high porous silicon layer. A refractive index of 2.35 corresponds to an initial porosity of 55% compared to 66% for the 2.05 case. Figure 7 demonstrates that the 2.05/3.05 combination has a strong influence on both the maximum achievable reflectance (99.1%) as well as on the stop-gap. The latter has increased to 300 nm (825–1125 nm).

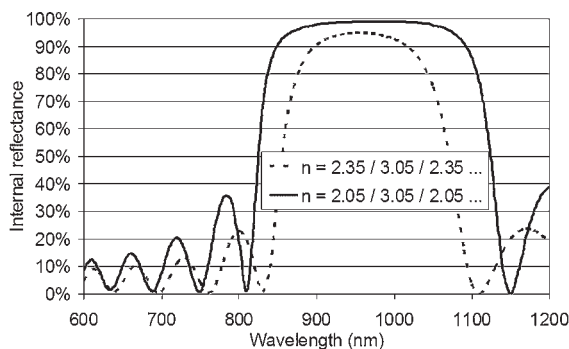


Figure 7. Internal reflectance at epi/substrate interface with two different 15-layer porous silicon stacks (alternating refractive indices of 2.35/3.05 and 2.05/3.05)

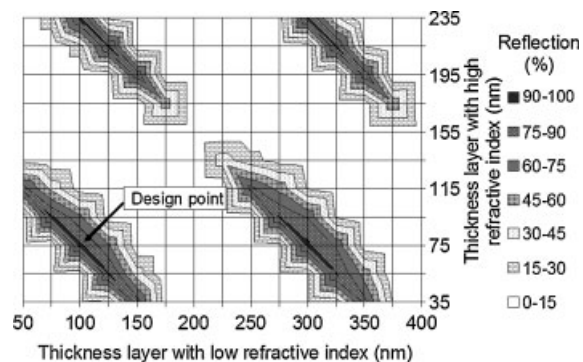


Figure 8. Influence of thickness of layers with low and high refractive index on the internal reflectance of an epi/reflector/substrate structure at the design wavelength of 950 nm (15 layer porous Si reflector)

Due to the speed and user-friendliness of the ART software, it is also straightforward to conduct a sensitivity analysis (Figure 8). The achievable efficiency at the design wavelength is plotted as function of the thickness of the layers with low and high refractive index. The graph clearly illustrates the interference effects: High reflectances are achieved at the design point (depicted by an arrow) and also at three times the design thickness for both layer types, which is the second order of constructive interference. The latter condition, however, has the disadvantage of a strongly reduced stop-gap (three times narrower than for the 1st order). At two times the design thickness, which is the 1st order condition for destructive interference, the reflectance reaches its minimum (0%). Concerning sensitivity, this graph, when zoomed, indicates that an error of ± 10 nm around the design point can be allowed while keeping the reflectance above 90%.

In the aforementioned examples, the number of layers was chosen as an odd number and the top layer (=the one closest to the epitaxial layer) has a low

refractive index. Both these conditions are optimal. A reflector stack with a high refractive index as top layer will have a slightly lower maximum reflectance. This is related to the fact that in that case the transition from epitaxial silicon to the reflector stack is optically smoother ($n_{\text{Si}} \rightarrow n_{\text{High}} \rightarrow n_{\text{Low}}$) resulting in a lower reflectance compared to the other case ($n_{\text{Si}} \rightarrow n_{\text{Low}} \rightarrow n_{\text{High}}$) which has a stronger optical effect. For similar reasons, it is beneficial to have an odd number of layers. In this case and assuming a low refractive index as top layer, the bottom layer will also have a low refractive index, giving the desired effect. An even number layers will have a high refractive index as bottom layer, which is again optically speaking a smoother transition and therefore less appropriate. So at least theoretically, it is preferable to have a high porosity top layer but it also has to be recognized that this could lead in practice to a lower quality epitaxial layer. Nevertheless, experiments have shown that a similar epitaxial quality can be achieved on top of reorganized low and high porosity layers if sufficient care is taken during the reorganization step. The aim is to achieve a closure of the surface before epitaxial growth.

The combination of an odd number of layers and a low refractive index as top layer is also the only one for which all layers should follow the quarter-wavelength rule (see Equation (1)). In the three other possible cases, the top and/or bottom layer should have a thickness corresponding to $\lambda/2n$ for optimal internal reflectance (Table II). This is caused by phase shifts of 180° which occur at a transition from a low to high refractive index material but which are absent for transitions from high to low refractive index.

For all the previous simulations, the incidence angle of the rays was 0° , in other words perpendicular to the epi/reflector interface. However, the front surface of efficient epitaxial cells is textured with the aim of reducing the surface reflection and limiting the specular component in the refracted light. In our

Table II. Ideal optical thickness of the individual layers in a multiple layer Bragg reflector depending on the refractive index of the adjacent layers (structure = epitaxial Si/multiple reflector layer/Si substrate)

| Top layer of reflector stack | Number of layers in stack | Ideal optical thickness top layer | Ideal optical thickness bottom layer | Ideal optical thickness other layers |
|------------------------------|---------------------------|-----------------------------------|--------------------------------------|--------------------------------------|
| Low refractive index | Odd | $\lambda/4$ | $\lambda/4$ | $\lambda/4$ |
| Low refractive index | Even | $\lambda/4$ | $\lambda/2$ | $\lambda/4$ |
| High refractive index | Odd | $\lambda/2$ | $\lambda/2$ | $\lambda/4$ |
| High refractive index | Even | $\lambda/2$ | $\lambda/4$ | $\lambda/4$ |

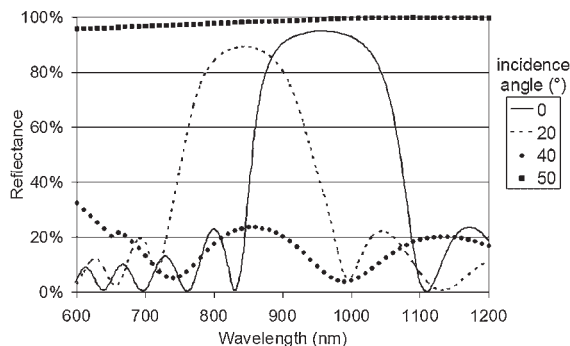


Figure 9. Effect of the incidence angle on the reflectance properties of a 15-layer porous Si stack

technology, this is achieved by plasma texturing using a fluorine plasma.¹⁸ Ideally, this texturing gives the front surface a lambertian character so that the angular distribution of the rays inside the epitaxial layer is uniform across all angles. In that case, a large portion of the rays will strike the epi/reflector interface at angles for which the Bragg reflector is not optimal anymore. The reflected light as a function of the incident angle for the epi/reflector/substrate structure is shown in Figure 9. The angular behaviour shows three distinct regions:

- For incidence angles near the normal ($\sim 0^\circ$), the reflector works sufficiently well as a Bragg reflector in the required wavelength range. At small angles (e.g. 20° , see Figure 9), the response has shifted to smaller wavelengths and therefore the efficiency of the Bragg reflector is reduced.
- For oblique incident angles ($\geq 45^\circ$), the rays strike at an angle larger than the critical angle for the interface between the epitaxial layer and the top layer with low refractive index. In this case, total internal reflection (TIR) occurs and the effective reflection nears 100%.
- At intermediate angles, the reflection drops to low levels. The reason for this is twofold: (i) The rays move at different angles through the layers with low and high refractive index. This means that for higher incident angles ($> 20^\circ$), the Bragg condition is not fulfilled anymore. (ii) Around the critical angle, which is approximately 41° for transition from Si to a layer with a refractive index of 2.35, frustrated TIR¹⁹ can occur. Evanescent waves with an exponentially decaying electric field perpendicular to the interface can leak energy through a thin dielectric layer akin to electromagnetic tunnelling. It is for this

reason that the reflection does not become 100% for angles slightly above the critical angle. Thicker layers will be less sensitive to this effect since this 'optical tunnelling' is very dependent on the thickness of the layers.

If the angular distribution of the light is completely equal for all angles, 50% of all photons would strike the interface at an angle greater than 60° .²⁰ From these considerations, it can be deduced that TIR is the most important effect of the reflector. Although the creation of a lambertian-like surface is feasible by plasma texturing, it would be at the cost of a considerable removal of epitaxial silicon. In practice, a good texturing can be achieved with a limited Si removal of only $1 \mu\text{m}$. In this case, there remains a considerable specular component in the refracted light. Therefore, the Bragg and the TIR effect both play an important role in the reflection at the epi/reflector interface. The impact of both is illustrated in Figure 10 which gives a comparison in measured external reflectance between textured epitaxial cells with a 15-layer porous silicon reflector and a single layer reflector. The TIR effect in both cases is expected to be similar since both reflectors have the same top layer. From the figure it is clear that the 15-layer reflector brings an additional boost due to the Bragg effect. The internal reflectance, calculated for these measured curves, at wavelengths above 1000 nm is 55% for the single layer reflector (i.e. TIR) and 80% for the 15-layer reflector (=TIR + Bragg effect). In other words, the Bragg effect contributes 25% to the internal reflection of 80%. At very long wavelengths, above the window of the Bragg reflection, both curves show a similar

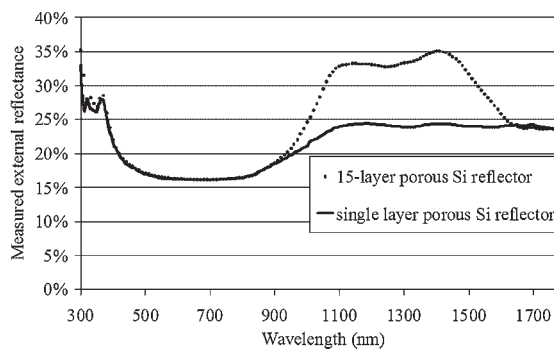


Figure 10. Effect of total internal reflection (single layer porous Si reflector) versus combined Bragg and TIR effect (15-layer porous Si reflector) for textured epitaxial surfaces

reflectance. This confirms that the contribution from the TIR effect is the same for both reflectors.

POTENTIAL OF AN EPITAXIAL SILICON SOLAR CELL

Screenprinted epitaxial solar cells including a reflector have shown boosts in short-circuit current of 2–3 mA/cm². The solid line in Figure 11 shows the expected current increase as function of wavelength if it were possible to fabricate a perfect internal reflector (i.e. internal rear reflection of 100%). This analysis is based on the AM1.5G spectrum which explains the dip around 930 nm since the spectrum has a low power density around that wavelength. The assumed Si epitaxial thickness for this calculation is 17 μm. The front surface is textured with a single anti-reflection coating (75 nm of SiN_x). The internal quantum efficiency of a real epitaxial cell is used as an input. The internal reflection at the front surface is taken as 93% which is the approximate value for lambertian light striking a Si/air interface. As stated above, a perfect reflector is assumed for the solid line represented in Figure 11. Integrated, this represents a current increase of 4.5 mA/cm². While such a perfect reflector is out of reach, we believe that, based on our current achievements, the realization of a reflector with an efficiency of 95% is likely. The dashed line in the same figure represents the porous silicon reflector with refractive indices of 2.05/3.05 as explained in the Section ‘Simulation of a Porous Silicon Intermediate Reflector’. Although there are clearly some losses compared to the ideal case, this still integrates to an achievable current increase of 3.9 mA/cm².

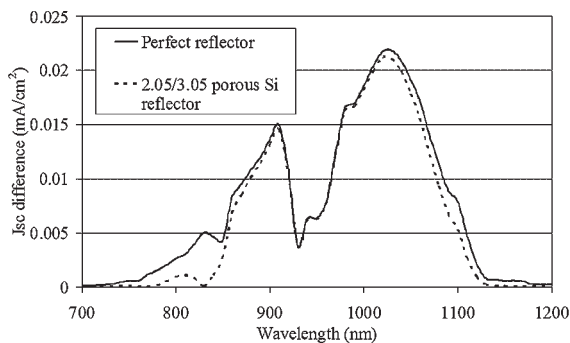


Figure 11. Benefit in short-circuit current by use of a perfect internal reflector (100% internal reflection) and a realistically achievable reflector

On the other hand, the epitaxial process offers a very large freedom in the creation of the doping profile for the base and emitters of the cells. Unlike the typical Gaussian or error function profile of a diffused emitter, the epitaxial process allows the creation of a profile specifically designed to boost the collection of short-wavelength photons. This has been shown recently by our work on emitter CVD processes (Van Nieuwenhuysen K, Duerinckx F, Kuzma-Filipek I, Recaman Payo M, Beaucarne G, Poortmans J. Epitaxially grown emitters for thin film crystalline silicon solar cells. *Thin Solid Films*, unpublished work) for which we have shown IQE measurements close to 100% at very short wavelengths (350–500 nm). This has resulted in lab-type efficiencies close to 15% for small epitaxial cells. Another example of this design freedom is the possibility of a graded profile in the base of the cell to drive the minority carriers towards the junction.

After some more development time, we expect that these different scientific achievements can be combined to improve the status of the current epitaxial cells. Screen-printed epitaxial solar cells on low quality silicon substrates with short-circuit currents of 32 mA/cm² and efficiencies of 15–16% seem within reach in a few years of time.

CONCLUSION

The inclusion of a porous silicon-based internal reflector for epitaxial crystalline silicon solar cells led to an efficiency improvement of more than 1% absolute. Top efficiencies for screenprinted epitaxial cells of 13.8% (18 cm² on highly doped mono-Si substrate) and 13.1% (71 cm² on highly doped UMG-Si substrate) have been obtained. A user friendly and powerful optical simulation tool has been presented that is instrumental in the understanding and scheduled further optimization of the internal reflector. It has been shown that the ratio of the refractive indices of the individual layers is extremely important not only for increasing the internal reflection but also especially for widening the wavelength window. A sensitivity analysis has shown an allowable deviation of 10 nm from the design thickness. Three separate working regimes, depending on the incident light angle, have been found including a Bragg regime (small incident angles) and a region where TIR (high incident angles) is dominant. These findings are a blueprint for the development of internal reflectors

with efficiencies above 90%. It is predicted that this further optimization, together with other developments on the level of the epitaxial process itself, will culminate in epitaxial cells with efficiencies of 15–16% in the near future.

Acknowledgements

The authors thank Mr D. Dehertoghe for his assistance during processing. The financial support from the European Community is acknowledged for the FP6 project Crystal Clear (Project No. SES6-CT-2003-502583).

REFERENCES

1. Agostinelli G, Choulat P, Dekkers HFW, Ma Y, Beaucarne G. Silicon solar cells on ultra-thin substrates for large scale production. *Proceedings of 21st European PVSEC*, Dresden, 2006; 601–604.
2. Duerinckx F, Kuzma-Filipek I, Van Nieuwenhuysen K, Beaucarne G, Poortmans J, Leloup F, Versluys J, Hanselaer P. Optical path length enhancement for >13% screenprinted thin film silicon solar cells. *Proceedings of 21st European Photovoltaic Solar Energy Conference*, Dresden, Germany, September, 2006; 726–729.
3. Van Nieuwenhuysen K, Van Gestel D, Kuzma I, Duerinckx F, Kim H, Beaucarne G, Poortmans J. Characterization of thin silicon films grown in a Batch-type LPCVD system. *Proceedings of 20th European Photovoltaic Solar Energy Conference and Exhibition*, Barcelona (Spain), 2005; 1251–1254.
4. Reber S, Hurrle A, Eyer E, Willeke G. Crystalline thin film solar cells—recent results at Fraunhofer ISE. *Solar Energy* 2004; **77**(6): 865–875.
5. Ma LL, Zhou YC, Jiang N, Lu X, Shao J, Lu W, Ge J, Ding XM, Hou XY. Wide-band “black silicon” based on porous silicon. *Applied Physics Letters* 2006; **88**: 171907.
6. Zeng L, Yi Y, Hong C, Liu J, Feng N, Duan X, Kimerling LC, Alamarium BA. Efficiency enhancement in Si solar cells by textured photonic crystal back reflector. *Applied Physics Letters* 2006; **89**: 111111.
7. Mazzoleni C, Pavesi L. Application to optical components of dielectric porous silicon multilayers. *Applied Physics Letters* 1995; **67**(20): 2983–2985.
8. Diener J, Künzner N, Kovalev D, Gross E, Timoshenko VY, Polisski G, Koch F. Dichroic Bragg reflectors based on birefringent porous silicon. *Applied Physics Letters* 2001; **78**(24): 3887–3889.
9. Van Nieuwenhuysen K, Duerinckx F, Kuzma I, Van Gestel D, Kim H, Beaucarne G, Poortmans J. Progress in epitaxial deposition on low-cost substrates for thin-film crystalline silicon solar cells at IMEC. *Journal of Crystal Growth* 2006; **287**: 438–441.
10. Müller G, Brendel R. Simulated annealing of porous silicon. *Physica Status Solidi A* 2000; **182**: 313–318.
11. Duerinckx F, Van Nieuwenhuysen K, Kim H, Kuzma-Filipek I, Dekkers H, Beaucarne G, Poortmans J. Large area epitaxial silicon solar cells based on industrial screen printing processes. *Progress in Photovoltaics: Research and Applications* 2005; **13**: 673–690.
12. Ghannam M, Abouelsaoud A, Kuzma I, Duerinckx F, Poortmans J. Optical modeling of capped multi-layer porous silicon as a back reflector in thin-film solar cells. *Proceedings of the IEEE 4th World Conference on Photovoltaic Energy Conversion*, Hawaii, 2006; 1362–1364.
13. Kuzma-Filipek I, Duerinckx F, Van Nieuwenhuysen K, Beaucarne G, Poortmans J, Mertens R. Porous silicon as a reflector in thin epitaxial silicon solar cells. *Physica Status Solidi A* 2007; **204**(5): 1340–1345.
14. Klein M, Furtak TE. *Optics*, 2nd edition. Wiley: New York, 2001; 295–300.
15. Vasicek A. Sur la réflexion de la lumière sur des verres supportant des couches minces multiples. *Journal de Physique et le Radium*, 1950 **tom 11**: 342–345.
16. Heavens OS. Optical properties of thin films. *Reports on Progress in Physics* 1960; **23**: 1–65.
17. Brendel R. Sunrays 1.3, distributed by Garching Innovation GmbH.
18. Dekkers H, Agostinelli G, Dehertoghe D, Beaucarne G, Traxlmayr U, Walther G. Improved performances of mc-Si solar cells by isotropic plasma texturing, 19th European Photovoltaic Solar Energy Conference and Exhibition, Paris (France), 2004; 412–415.
19. Klein MV, Furtak TE. *Optics*, 2nd edition. Wiley: New York, 2001; 85–86.
20. Campbell P, Green MA. Light trapping properties of pyramidally textured surfaces. *Journal of Applied Physics* 1987; **62**(1): 243–249.